Enhancing multi-bioreactor platforms for automated measurements and reactive experiment control

*François Bertaux[1,2 *†], Sebastián Sosa Carrillo[2,1,3 *], Achille Fraisse[2,1], Chetan Aditya[2,1,3], Mariela Furstenheim[1], Gregory Batt[2,1 †]*

1. Institut Pasteur, USR 3756 IP CNRS, 28 rue du Docteur-Roux, 75015 Paris, France
2. Inria Paris, 2 rue Simone Iff, 75012 Paris, France
3. Université Paris Diderot, Sorbonne Paris Cité, 12 rue de l'Ecole de Médecine, 75006 Paris, France

* These authors contributed to this work equally.
† Correspondence: francois.bertaux@pasteur.fr, gregory.batt@inria.fr

Abstract

New small-scale, low-cost bioreactor designs provide researchers with exquisite control of environmental parameters of microbial cultures over long durations, allowing them to perform sophisticated, high-quality experiments that are particularly useful in systems biology, synthetic biology and bioengineering. However, existing setups are limited in their automated measurement capabilities, primarily because sensitive and specific measurements require bulky, expensive, stand-alone instruments (for example, most single-cell resolved measurements require a cytometer or a microscope). We present here *ReacSight*, a generic and flexible strategy to enhance multi-bioreactor platforms for automated measurements and reactive experiment control. We use *ReacSight* to assemble a platform for single-cell resolved characterization and reactive optogenetic control of parallel yeast continuous cultures. We demonstrate its usefulness by achieving parallel real-time control of gene expression with light in different bioreactors and by exploring the relationship between fitness, nutrient scarcity and cellular stress density using highly-controlled and informative competition assays.

Introduction

Small-scale, low-cost bioreactors are emerging as powerful tools for microbial systems and synthetic biology research[1–4]. They allow tight control of cell culture parameters (e.g. temperature, cell density, media renewal rate) over long durations (many cell generations). These unique features enable researchers to perform sophisticated experiments and to achieve high experimental reproducibility. Examples include characterization of antibiotic resistance when drug selection pressures increases as resistance evolves[1], cell-density controlled characterization of cell-cell communication synthetic circuits[2], and genome-wide characterization of yeast fitness under dynamically changing temperature using a pooled knockout library[3].

A weakness of existing small-scale, low-cost bioreactors is their limited automated measurement capabilities: in situ optical density measurements only inform about overall biomass concentration and its growth rate, and when available[2,4] fluorescence measurements suffer from low sensitivity and high background. To quantify other key characteristics of the cell population under study (e.g. gene expression levels, cellular stress levels, cell size and morphology, cell cycle progression, proportions of different genotypes/phenotypes), researchers usually need to manually extract, process and measure culture

samples to run them through more sensitive and specialized instruments (e.g. a cytometer, a microscope, a sequencer). This is usually tedious and strongly constrains the available temporal resolution and scope (i.e. no time-points during night-time). It also precludes the dynamic adaptation of culture conditions in response to such measurements (*reactive experiment control*). This would be useful to either maintain a certain state of the population (*external feedback control*) or to maximize the value of the experiment (*reactive experiment design*). For example, external feedback control can be used to disentangle complex cellular couplings and signaling pathway regulations[5–8], to steer the composition of microbial consortia[9] or to optimize industrial bioproduction[10]. Reactive experiment design can be especially useful in the context of long and uncertain experiments such as artificial evolution experiments[11].

In principle, commercial robotic equipment and/or custom hardware can be used to couple a multi-bioreactor setup to a sensitive, multi-sample (typically accepting 96-well plates as input) measurement device. However, this poses tremendous challenges regarding equipment sourcing, equipment cost and software integration, and very few examples have been reported. For instance, only two groups have demonstrated automated cytometry and reactive optogenetic control of bacteria[12] and yeast[6,7] cultures, with setups limited to either a single continuous culture or multiple batch-only cultures.

Here, we present *ReacSight*, a generic and flexible strategy to enhance multi-bioreactor platforms for automated measurements and reactive experiment control. We first use *ReacSight* to assemble a platform enabling single-cell resolved characterization and reactive optogenetic control of parallel yeast continuous cultures. We then demonstrate its usefulness on two case studies. First, we achieve parallel real-time control of gene expression with light in different bioreactors. Second, we explore the relationship between fitness, nutrient scarcity and cellular stress density using highly-controlled and informative competition assays.

Results

Measurement automation, platform software integration and reactive experiment control with *ReacSight*

The *ReacSight* strategy (Figure 1, Text S1.1) to enhance multi-bioreactor platforms for automated measurements and reactive experiment control combines hardware and software elements. A pipetting robot is used to establish, in a generic fashion, a physical link between any multi-bioreactor setup and any plate-based measurement device (Figure 1, left). Bioreactor culture samples are sent to the pipetting robot through pump-controlled sampling lines attached to the robot arm (*sampling*). A key advantage of using a pipetting robot is that treatment steps can be automatically performed on culture samples before measurement (*treatment)*. Samples are then transferred to the measurement device by the pipetting robot (*loading*), thanks to a positioning of the device such that upon loading tray opening, part or all of the device input plate is accessible to the robot. Partial access to the device input plate is not problematic because the robot can be used to wash input plate wells between measurements, allowing re-use of the same wells over time (*washing*). Importantly, if reactive experiment control based on measurements is not needed, the robot capabilities can also be used to treat and store culture samples for one-shot offline measurements at the end of an experiment, enabling automated dynamic measurements with flexible temporal resolution and scope.

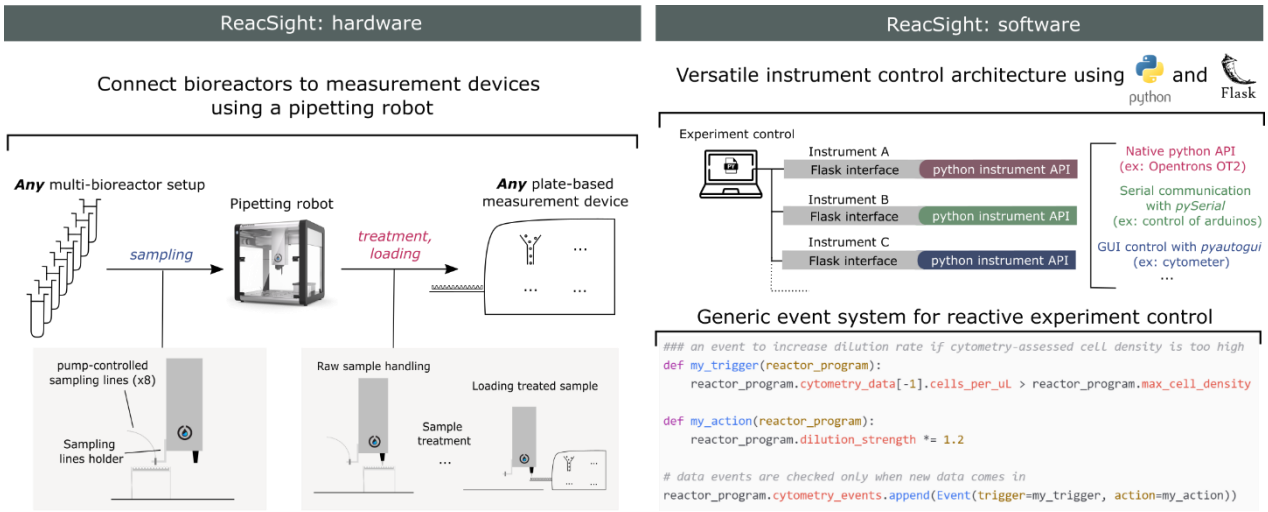

Figure 1. ***ReacSight: a strategy to enhance multi-bioreactor platforms for automated measurements and reactive experiment control****. On the hardware side, ReacSight leverages a pipetting robot (such as the low-cost, open-source Opentrons OT-2) to create a physical link between any multi-bioreactor setup (eVOLVER, Chi.Bio…) and the input of any plate-based measurement device (plate reader, cytometer, high-throughput microscope, pH-meter…). Sampling tubing lines are attached to the robot arm using a custom-fabricated Plexiglas piece. If necessary, the pipetting robot can be used to perform a treatment on bioreactor samples (dilution, fixation, extraction, purification…) before loading into the measurement device. If reactive experiment control is not needed, treated samples can also be stored on the robot-deck for offline measurements (the OT-2 temperature module can help the conservation of temperature-sensitive samples). On the software side, ReacSight enables full platform integration via a versatile instrument control architecture based on python and the python web application framework Flask. ReacSight software also provides a generic event system to enable reactive experiment control. Example code for a simple use case of reactive experiment control is shown.*

ReacSight also provide a solution to several software challenges that should be addressed to unlock automated measurements and reactive experiment control of multi-bioreactors (Figure 1, right). First, programmatic control of all instruments of the platform (bioreactors, pipetting robot, measurement device) is required. Second, a single computer should communicate with all instruments to orchestrate the whole experiment. *ReacSight* combines the versatility and power of the *python* programming language with the genericity and scalability of the *Flask* web-application framework to address both challenges. Indeed, *python* is ideally suited to easily build APIs to control various instruments: there exist well-established, open-source libraries for the control of micro-controllers (such as arduinos), and even of GUI-only software (*pyautogui*) for closed-source instruments lacking APIs. Importantly, the open-source, low-cost pipetting robot OT-2 (*Opentrons*) is shipped with a native python API. Flask can then be used to expose all instrument APIs for simple access over the local network. The task of orchestrating the control of multiple instruments from a single computer is then essentially reduced to the simple task of sending HTTP requests, for example using the python module *requests.* Finally, in addition to this versatile instrument control architecture, *ReacSight* provides a generic object-oriented implementation of *events* (if *this* happens, do *this*) to facilitate reactive experiment control. Key software elements as well as source files for hardware pieces are available in the *ReacSight* Git repository.

Reactive optogenetic control and single-cell resolved characterization of yeast continuous cultures

Our first application of the *ReacSight* strategy is motivated by yeast synthetic biology applications. Being able to 1) accurately control synthetic circuits and 2) measure their output in well-defined cellular and environmental contexts and with sufficient temporal resolution and scope is critical in this context. Optogenetics provides an ideal way to control synthetic circuits, and bioreactor-enabled continuous

cultures are ideal to exert tight control over growth conditions for long durations. To measure circuit output in single cells, cytometry is also ideal due to high sensitivity and throughput. We thus resorted to the *ReacSight* strategy to assemble a fully automated experimental platform enabling reactive optogenetic control and single-cell resolved characterization of yeast continuous cultures (Figure 2A), using a benchtop cytometer as a measurement device.

Detailed information on the platform hardware and software is provided in Text S1.2, and we discuss here only key elements. Eight reactors are connected to the pipetting robot, meaning that each timepoint fills one row of a sampling plate. While three rows of the cytometer input plate are accessible by the robot, we use only one row, washed extensively by the robot to achieve less than 0.2% carry-over as validated using beads. We typically fit two tip boxes and two sampling plates on the robot deck, therefore enabling 24 x 8 timepoints without any human intervention. To enable reactive experiment control based on cytometry data, we developed and implemented algorithms to perform automated gating and spectral deconvolution between overlapping fluorophores (Figure 2B).

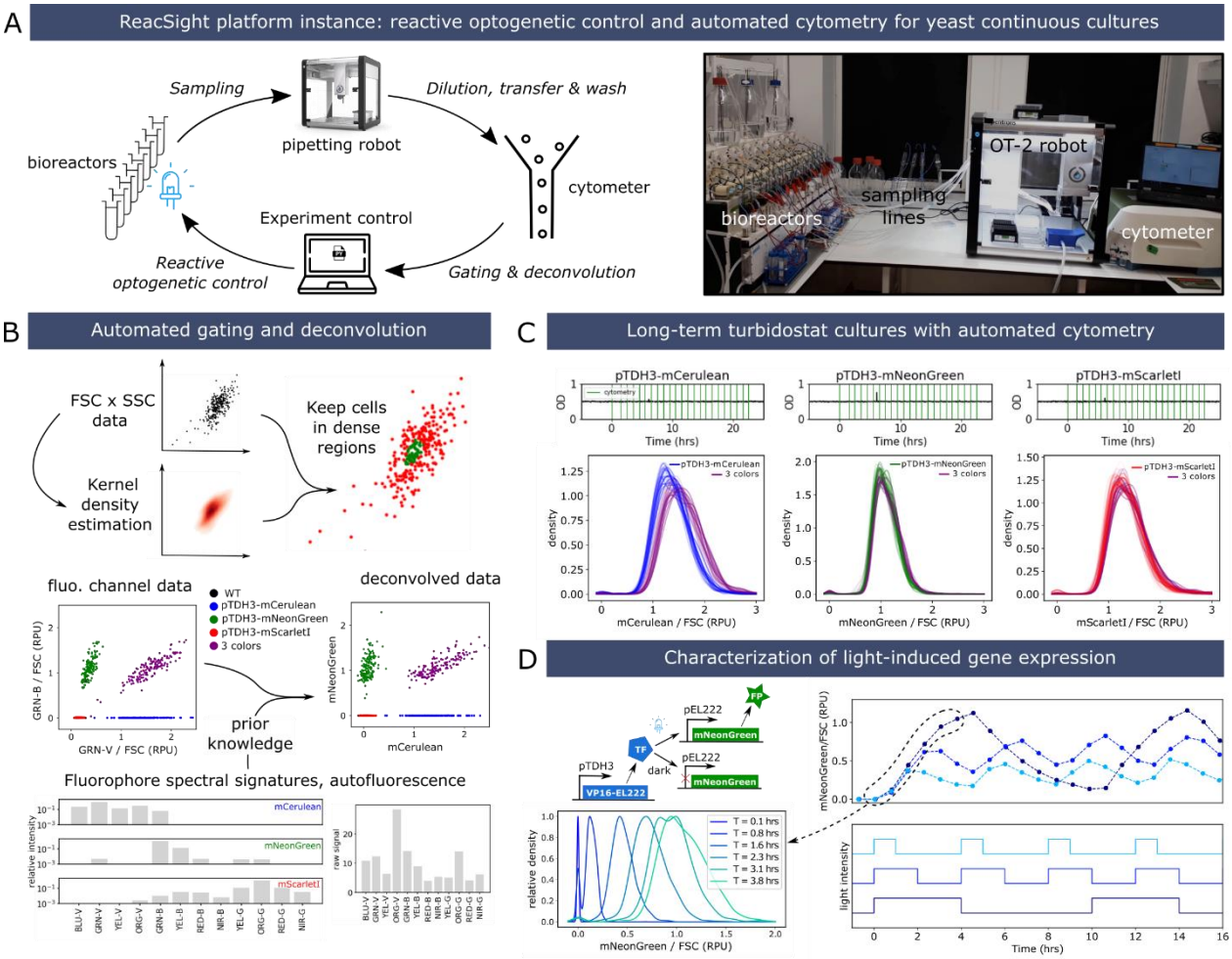

Figure 2. ***ReacSight-based assembly of a fully automated platform enabling reactive optogenetic control and single-cell resolved characterization of yeast continuous cultures.*** *(A) Platform overview. The Opentrons OT-2 pipetting robot is used to connect optogenetic-ready multi-bioreactors to a benchtop cytometer (Guava EasyCyte 14HT, Luminex). The robot is used to dilute fresh culture samples in the cytometer input plate and to wash it between timepoints. The 'clicking' python library pyautogui is used to*

create the cytometer instrument control API. Custom algorithms were developed and implemented in python to automatically gate and deconvolve cytometry data on the fly. (B) Description of the gating and deconvolution algorithm. As an example, deconvolution between the overlapping fluorophores mCerulean and mNeonGreen are shown. (C) Stability of single-cell gene expression distributions over many generations. Strains constitutively expressing either mCerulean, mNeonGreen or mScarlet-I alone or altogether ('3-colors' strain) from the transcriptional units driven by the pTDH3 promoter and integrated in the chromosome were grown in turbidostat mode (OD setpoint = 0.5, upper plots) and cytometry was acquired every hour. Distributions of fluorophore levels (after gating, deconvolution, and normalization by the forward scatter, FSC) for all timepoints are plotted together with different color shades (bottom). RPU: relative promoter units (see Methods). (D) Characterization of a light-driven gene expression circuit based on the EL222 system[13]. Three different ON-OFF blue light temporal profiles were applied (bottom) and cytometry was acquired every 45 minutes. The median of gated, deconvolved, FSC-normalized data is shown (top). All bioreactor experiments presented in this figure were performed in parallel, the same day.

We first validated the performance of the platform by performing long-term turbidostat cultures of yeast strains constitutively expressing various fluorescent proteins from chromosomally integrated transcriptional units (Figure 2C). Distributions of fluorophores levels were unimodal and stable over time, as expected from steady growth conditions with a constitutive promoter. Distributions of *mNeonGreen* and *mScarlet-I* exactly overlapped between the single- and 3- color strains, as expected from the assumptions that expressing one or three fluorescent proteins from the strong *pTDH3* promoter has negligible impact on cell physiology and that the relative positioning of transcriptional units in the 3-color strain (*mCerulean* first, followed by *mNeonGreen* and *mScarlet-I*) has little impact on gene expression. Measured levels of *mCerulean* appear slightly higher (~15%) in the 3-color strain compared to the single-color strain. This could be caused by residual errors in the deconvolution, exacerbated by the low brightness of *mCerulean* compared to autofluorescence and to *mNeonGreen*.

Finally, to validate the optogenetic capabilities of the platform, we built and characterized a light-inducible gene expression circuit based on the EL222 system[13] (Figure 2D). As expected, applying different ON-OFF temporal patterns of blue light resulted in dynamic profiles of fluorophore levels covering a wide range, from near-zero levels (i.e., hardly distinguishable from auto-fluorescence) to levels exceeding those obtained with the strong constitutive promoter *pTDH3*. Cell-to-cell variability in expression levels at high induction is also low, with CV (coefficient of variation) values comparable to the *pTDH3* promoter (0.22 vs 0.20).

Real-time control of gene expression using light

To showcase the reactive optogenetic control capabilities of the platform, we set out to dynamically adapt light stimulation so as to maintain fluorophore levels at different target setpoints. Such in-silico feedback for in-vivo regulation of gene expression is useful to dissect the functioning of endogenous circuits in the presence of complex cellular regulations and could facilitate the use of synthetic systems for biotechnological applications[6,10,14].

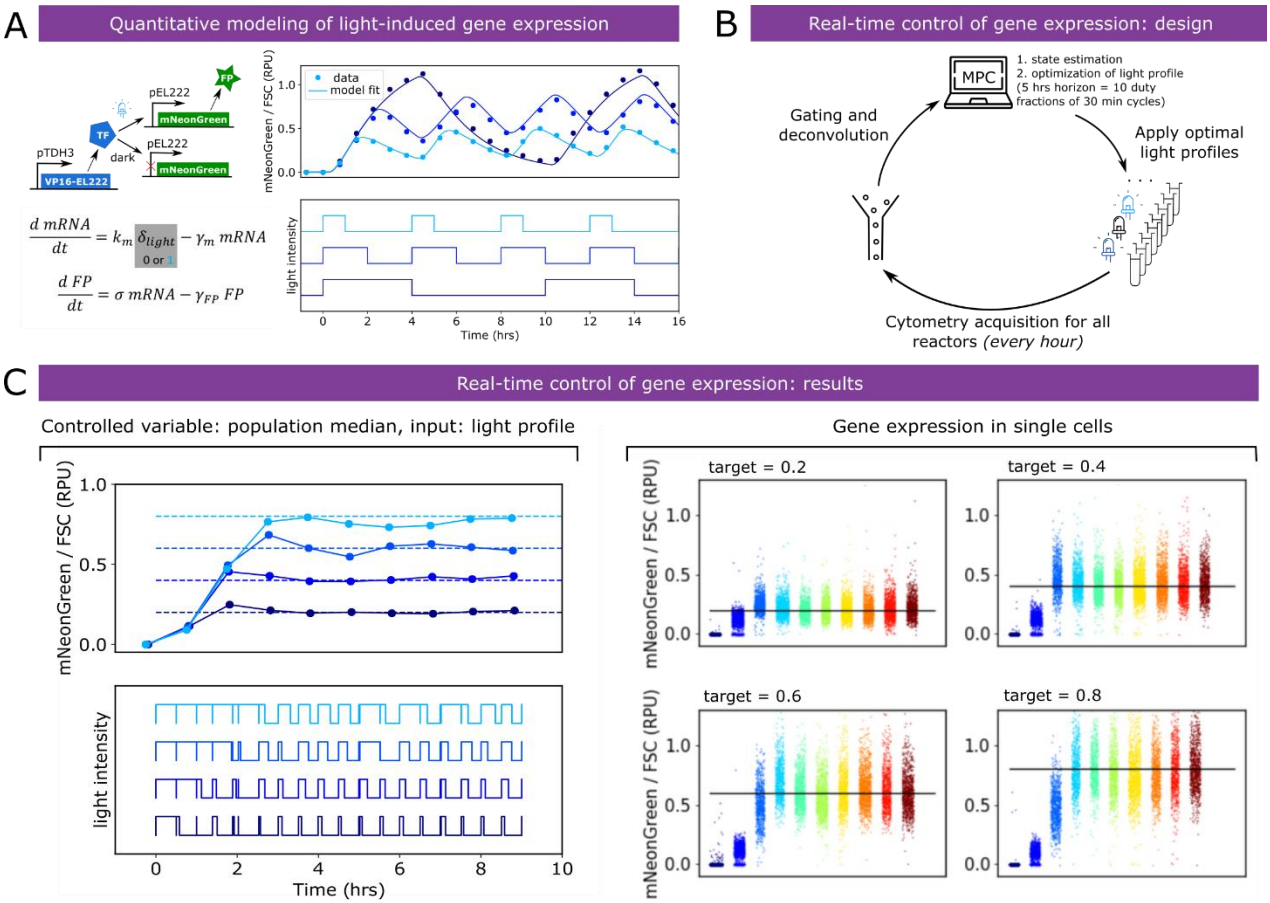

Figure 3. ***Closing the loop: real-time control of gene expression using light.*** *(A) A simple ODE model of the light-driven gene expression circuit is fitted to the characterization data of Figure 2D. Fitted parameters are* $\gamma_m = 2.09\ hr^{-1}$, $\sigma = 0.64\ RPU.hr^{-1}$ *and* $\gamma_{FP} = 0.475\ hr^{-1}$. k_m *was arbitrarily set to equal* γ_m *to allow parameter identifiability from protein median levels only. (B) Description of real-time control of gene expression experiments. Every hour, cytometry acquisition is performed, and after gating, deconvolution and FSC-normalization the data is fed to a model-predictive control (MPC) algorithm. The algorithm uses the model to search for the best sequence of duty fractions for 10 duty cycles of period 30 minutes (i.e. a horizon of 5 hours) in order to track the target level. (C) Real-time control results for four different target levels, performed in parallel in different bioreactors. Left: median of single cells (controlled value). Right: single-cell distributions over time. Note that a linear scale is used on all plots.*

We first constructed and validated a simple mathematical model of light-induced gene expression (Figure 3A). Joint fitting of the three model parameters to the characterization data of Figure 2D resulted in an excellent quantitative agreement. This gives further confidence in the ability of the platform to provide reproducible and reliable quantitative data. We then incorporated the fitted model into a model-predictive control algorithm (Figure 3B). Together with the *ReacSight* event system, this algorithm enabled accurate real-time control of fluorophore levels to different targets in different reactors in parallel (Figure 3C).

Exploring the relationship between fitness, nutrient scarcity and cellular stress

A key advantage of using cytometry to characterize bioreactor cultures is the possibility to phenotype single cells, and even to genotype them if different strains harbor distinct fluorescent barcodes. This capability unlocks a new class of experiments: multiplexed strain characterization and competition in dynamically controlled environments (Figure 4A). Indeed, some fluorophores can be used for genotyping and others for phenotyping. Automated cytometry (including raw data analysis) will then provide

quantitative information on both the competition dynamics between the different strains and cell state distribution dynamics for each strain. Depending on the goal of the experiment, this rich information can be fed back to experiment control to adapt environmental parameters for each reactor.

As a proof of concept that such experiments can be carried out, we set out to explore the relationship between fitness, nutrient scarcity and cellular stress (Figure 4B, top-left). Different species in microbial communities have different nutritional needs depending on their metabolic diversity or specialization, and their fitness therefore depends not only on external environmental factors but also on the community itself through nutrient consumption, metabolite release, and other inter-cellular couplings[15,16]. As opposed to competition assays in batch, continuous culture allows to control for such factors. For example, in turbidostat cultures, nutrient availability depends on both nutrient supply (i.e. nutrient levels in the input medium) and nutrient consumption by cells (which primarily depends on the OD setpoint). We used histidine auxotrophy as a model for nutrient scarcity: for *his3* mutant cells, histidine is an essential nutrient. By competing *his3* mutant cells with wild-type cells at different OD setpoints and different histidine concentrations in the input medium, we can measure how nutrient scarcity affects fitness (Figure 4B, top-right). Using a stress reporter in both strains also informs about the relationship between fitness and cellular stress in the context of nutrient scarcity. We focused on the UPR (Unfolded Protein Response[17]) stress response to investigate whether nutrient stress can lead to other, a priori unrelated types of stress, which will be indicative of global couplings in cell physiology.

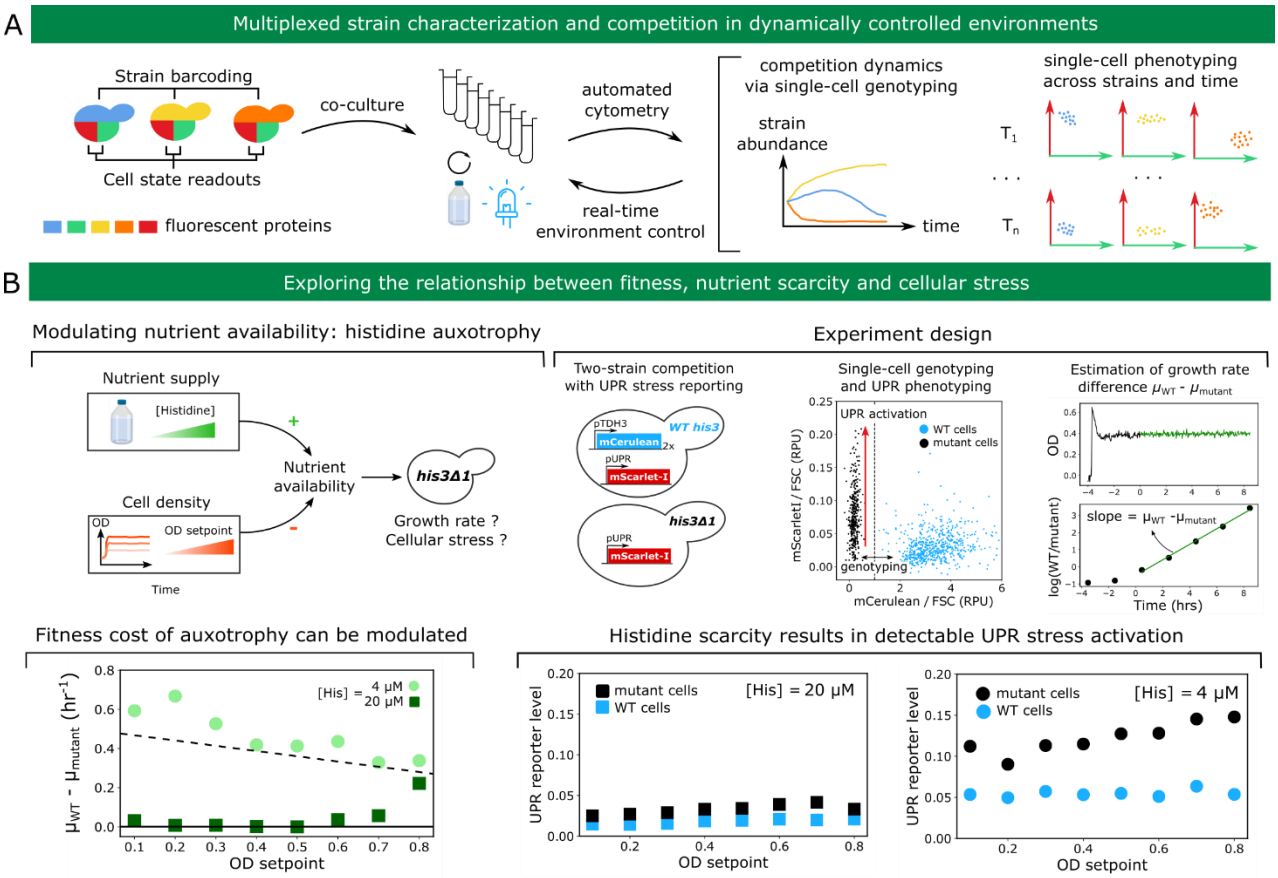

Figure 4. ***Exploring the relationship between fitness, nutrient scarcity and cellular stress.*** *(A) Opening up a new class of experiments by combining co-cultures, automated cytometry for single-cell genotyping and phenotyping and reactive experiment control to adapt environmental conditions in real-time. (B) Top-left: the availability of essential nutrients (such as histidine for his3*

mutant strains) depends on the environmental supply but also on cell density via nutrient consumption. Low nutrient availability will impede growth rate and might trigger cellular stress. Top-right: experiment design. Wild-type cells (marked with mCerulean constitutive expression) are co-cultured with his3 mutant cells. Both strains harbor a UPR stress reporter construct driving expression of mScarlet-I. Automated cytometry enables to assign single cells to their genotype and to monitor strain-specific UPR activation. The dynamics of the relative amount of the two strains allows inference of the growth rate difference between mutant and wild-type cells for each condition. Bottom-left: cell density dependence of the fitness deficit of mutant cells at two different media histidine concentration. The dashed line indicates the approximate dependence of wild-type growth rate on the OD setpoint. Bottom-right: strain-specific UPR activation for each condition.

At a histidine concentration of 4 µM, *his3* mutant cells are strongly outcompeted by wild-type cells over the range of OD setpoints (0.1 – 0.8) we considered (Figure 4B, bottom-left). This is not the case anymore at a concentration of 20 µM: then, the growth rate advantage of wild-type cells is close to zero below an OD setpoint of 0.6 and becomes larger than 0.2 hr^{-1} at the largest OD setpoint of 0.8. Therefore, for this level of nutrient supply, levels of nutrient consumption by cells have a strong impact on fitness of *his3* mutant cells. This qualitative change between 4 µM and 20 µM is highly consistent with the reported value of 17 µM for the K_m constant of the single high-affinity transporter of histidine, *HIP1*[18]. Also, because the growth rate difference between wild-type and mutant cells for a histidine concentration of 4 µM is close or exceeds the typically observed growth rate of wild-type cells (between 0.3 and 0.45 hr^{-1} depending on the OD setpoint), we can conclude that mutant cells are growth-arrested in these conditions. Single-cell UPR phenotyping data shows little difference between mutant and wild-type cells across all OD setpoints for a histidine concentration of 20 µM but a clear activation of the UPR response in mutant cells at a histidine concentration of 4 µM (Figure 4B, bottom-right). Therefore, as opposed to growth arrest, growth rate reduction caused by nutrient scarcity does not lead to strong UPR activation.

Discussion

We report the development of *ReacSight*, a strategy to enhance multi-bioreactor setups with automated measurements and reactive experiment control. *ReacSight* addresses an unmet need by allowing researchers to combine the recent advances in low-cost, open-hardware instruments for continuous cultures of microbes (e.g. *eVOLVER, Chi.Bio*[3,4]) and multi-purpose, modular, programmable pipetting robots (e.g. *Opentrons OT-2*) with sensitive, but generally expensive, stand-alone instruments to build fully automated platforms that open up radically novel experimental capabilities. *ReacSight* is generic and easy to deploy, and should be broadly useful for the microbial systems biology and synthetic biology communities. While we deployed the *ReacSight* strategy for only one measurement device (a benchtop cytometer), it should be possible to position two devices on each side of the pipetting robot to enable even more advanced workflows.

As already noted by Wong and colleagues[3], connecting a multi-bioreactor setup to a cytometer for automated measurements could enable single-cell resolved characterization of microbial cultures across time. Automated cytometry in the context of microbial systems and synthetic biology has in fact already been demonstrated years ago by a small number of labs[6,12,19], but low throughput or reliance on expensive automation equipment likely prevented a wider adoption of this technology. Automated cytometry from continuous cultures becomes especially powerful in combination with recently developed optogenetic systems[20,21], enabling targeted, rapid and cost-effective control over cellular processes[12]. We demonstrated the key capabilities of such platform by performing parallel, light-driven real-time control of gene expression in different bioreactors as well as fully automated, cell-state informing competition assays in tightly controlled environmental conditions. While we used *ReacSight* to connect our own, pre-existing custom multi-bioreactor setup with a cytometer, it can instead be used in combination with the

recent *Chi.Bio* optogenetic-ready bioreactor system to build such platform at a small time and financial cost (excluding the cost of the cytometer, which are expensive but already widespread in labs given their broad usefulness even in absence of automation). We only touched the surface of the large space of potential applications offered by such platforms. Strain barcoding can be scaled-up to 10-15 strains (for example by integrating different copy numbers of two fluorophores driven by the same promoter, their ratio providing a readout of cell genotype). Such multiplexing capabilities can be especially useful to characterize the input-output response of various candidate circuits (or the dependence of circuit behavior across a library of strain backgrounds) in parallel (using different light inductions across reactors). Immuno-beads can be used for more diverse cytometry-based measurements (the robot enabling automated incubation and wash, for example using the *Opentrons OT-2* magnetic module). Technologies such as surface display[22,23] can also be used to engineer biosensor strains to measure even more dimensions of the cultures with a single cytometer and at no reagent costs.

In the future we hope that many *ReacSight*-based platforms will be assembled and their design shared by a broad community to drastically expand our experimental capabilities, in order to shed new light on fundamental questions in microbiology or to unlock the potential of synthetic biology in biotechnological applications.

Methods

Cloning and strain construction. All plasmids and strains are constructed from the common laboratory strain BY4741 using the modular cloning framework for yeast synthetic biology *Yeast Tool Kit* by Lee and colleagues[24]. All strains used express the light-inducible transcription factor from the *URA3* locus (transcriptional unit: *pTDH3 NLS-VP16-EL222 tSSA1*). Single-color constitutive expression strains (Figure 2) also harbor a *pTDH3 FP tTDH1* transcriptional unit at the *LEU2* locus where *FP* is *mCerulean*, *mNeonGreen* or *mScarlet-I*. Corresponding CDS have been codon-optimized for expression in *S. cerevisiae*. The three-color strain harbors the same three transcriptional units in tandem (order: *mCerulean*, *mNeonGreen*, *mScarlet-I*) at the *LEU2* locus. The autofluorescence strain harbors an empty cassette at the *LEU2* locus to match auxotrophy markers between strains. For light-inducible gene expression (Figure 2 and 3), a *pEL222 mNeonGreen tTDH1* transcriptional unit (where *pEL222* is composed of 5 copies of the EL222 binding site followed by a truncated *CYC1* promoter[13]) is integrated at the *LEU2* locus. For the histidine competition experiments, the mutant strain is simply BY4741 expressing the light-inducible transcription factor from the *URA3 locus,* i.e. the common parental strain for all strains used in this work, which is auxotroph for histidine, leucine and methionine. The wild-type strain was obtained from the mutant strain by integrating two identical *pTDH3 mCerulean tTDH1* transcriptional units in tandem at the *HO* locus with *HIS3* selection, thereby restoring histidine prototrophy and enabling fluorescent barcoding.

Cell culture conditions. All experiments were performed in 30 mL culture volume bioreactors (cf Text S1.2) at 30 degrees and in turbidostat mode (OD 0.5, typically corresponding to 10^7 cells/mL according to cytometry data) with synthetic complete medium (ForMedium LoFlo yeast nitrogen base CYN6510 and Formedium complete supplement mixture DCS0019) except for histidine competition experiment where histidine drop-out amino-acid mixture was used (Sigma Y1751) and complemented with desired levels of histidine (Sigma 53319).

Cytometry acquisition and raw data analysis. Gain settings of our cytometer (*Guava EasyCyte 14HT, Luminex*) for all channels were set once and for all prior to the study such that yeast auto-fluorescence under our typical growth conditions is detectable but at the lower end of the instrument 5-decade range.

We verified that cytometry data was reproducible week-to-week with those fixed settings. Single-color strains described above were used together with the autofluorescence control strain to obtain 'spectral' signatures of the three fluorophores *mCerulean*, *mNeonGreen* and *mScarlet-I* and autofluorescence levels for each channel. These signatures were also highly reproducible week-to-week. To convert raw cytometry data into fluorophore concentrations in relative promoter units (*RPU*[25]), we used a pipeline described in Text S2.2. This pipeline was implemented in *python* and is available in the *ReacSight* Git repository.

Histidine competition assays. Pre-cultures were performed in synthetic complete medium. Cells were washed in the same low histidine medium as the one used for turbidostat feeding of the competition culture and mixed with an approximate ratio mutant:WT of 5:1 (to ensure good statistics for long enough even when the mutant fitness is very low) before inoculation. Cytometry was acquired automatically every 2 hours. At steady-state, the ratio between two competitors in a co-culture evolves exponentially at a rate equals to their growth rate difference. Linearity of the ratio logarithm for at least 3 timepoints was therefore used to assess when steady-state is reached. A threshold of 1 *mCerulean RPU* was used to assign each cell to its genotype. Size gating was performed as described in Text 2.2 (parameters: size threshold = 0.5 and doublet threshold = 0.5, less stringent than for experiments of Figure 2 and 3) to discard dead or dying cells.

References

1. Toprak, E. *et al.* Evolutionary paths to antibiotic resistance under dynamically sustained drug selection. *Nat. Genet.* **44**, 101–105 (2012).
2. Takahashi, C. N., Miller, A. W., Ekness, F., Dunham, M. J. & Klavins, E. A Low Cost, Customizable Turbidostat for Use in Synthetic Circuit Characterization. *ACS Synth. Biol.* **4**, 32–38 (2015).
3. Wong, B. G., Mancuso, C. P., Kiriakov, S., Bashor, C. J. & Khalil, A. S. Precise, automated control of conditions for high-throughput growth of yeast and bacteria with eVOLVER. *Nat. Biotechnol.* **36**, 614–623 (2018).
4. Steel, H., Habgood, R., Kelly, C. & Papachristodoulou, A. In situ characterisation and manipulation of biological systems with Chi.Bio. *PLOS Biol.* **18**, e3000794 (2020).
5. Toettcher, J. E., Gong, D., Lim, W. A. & Weiner, O. D. Light-based feedback for controlling intracellular signaling dynamics. *Nat. Methods* **8**, 837–839 (2011).
6. Milias-Argeitis, A. *et al.* In silico feedback for in vivo regulation of a gene expression circuit. *Nat. Biotechnol.* **29**, 1114–1116 (2011).
7. Harrigan, P., Madhani, H. D. & El-Samad, H. Real-Time Genetic Compensation Defines the Dynamic Demands of Feedback Control. *Cell* **175**, 877-886.e10 (2018).
8. Lugagne, J.-B. & Dunlop, M. J. Cell-machine interfaces for characterizing gene regulatory network dynamics. *Curr. Opin. Syst. Biol.* **14**, 1–8 (2019).
9. Fedorec, A. J. H., Karkaria, B. D., Sulu, M. & Barnes, C. P. Single strain control of microbial consortia. *bioRxiv* 2019.12.23.887331 (2020) doi:10.1101/2019.12.23.887331.
10. Pouzet, S. *et al.* The Promise of Optogenetics for Bioproduction: Dynamic Control Strategies and Scale-Up Instruments. *Bioengineering* **7**, 151 (2020).
11. Zhong, Z. *et al.* Automated Continuous Evolution of Proteins in Vivo. *ACS Synth. Biol.* **9**, 1270–1276 (2020).
12. Milias-Argeitis, A., Rullan, M., Aoki, S. K., Buchmann, P. & Khammash, M. Automated optogenetic feedback control for precise and robust regulation of gene expression and cell growth. *Nat. Commun.* **7**, 12546 (2016).
13. Benzinger, D. & Khammash, M. Pulsatile inputs achieve tunable attenuation of gene expression variability and graded multi-gene regulation. *Nat. Commun.* **9**, 3521 (2018).

14. Chait, R., Ruess, J., Bergmiller, T., Tkačik, G. & Guet, C. C. Shaping bacterial population behavior through computer-interfaced control of individual cells. *Nat. Commun.* **8**, 1535 (2017).
15. Ghoul, M. & Mitri, S. The Ecology and Evolution of Microbial Competition. *Trends Microbiol.* **24**, 833–845 (2016).
16. Friedman, J. & Gore, J. Ecological systems biology: The dynamics of interacting populations. *Curr. Opin. Syst. Biol.* **1**, 114–121 (2017).
17. Travers, K. J. *et al.* Functional and Genomic Analyses Reveal an Essential Coordination between the Unfolded Protein Response and ER-Associated Degradation. *Cell* **101**, 249–258 (2000).
18. Bajmoczi, M., Sneve, M., Eide, D. J. & Drewes, L. R. TAT1 Encodes a Low-Affinity Histidine Transporter inSaccharomyces cerevisiae. *Biochem. Biophys. Res. Commun.* **243**, 205–209 (1998).
19. Zuleta, I. A., Aranda-Díaz, A., Li, H. & El-Samad, H. Dynamic characterization of growth and gene expression using high-throughput automated flow cytometry. *Nat. Methods* **11**, 443–448 (2014).
20. Liu, Z. *et al.* Programming Bacteria With Light—Sensors and Applications in Synthetic Biology. *Front. Microbiol.* **9**, (2018).
21. Figueroa, D., Rojas, V., Romero, A., Larrondo, L. F. & Salinas, F. The rise and shine of yeast optogenetics. *Yeast* yea.3529 (2020) doi:10.1002/yea.3529.
22. Park, M. Surface Display Technology for Biosensor Applications: A Review. *Sensors* **20**, 2775 (2020).
23. Shibasaki, S., Tanaka, A. & Ueda, M. Development of combinatorial bioengineering using yeast cell surface display—order-made design of cell and protein for bio-monitoring. *Biosens. Bioelectron.* **19**, 123–130 (2003).
24. Lee, M. E., DeLoache, W. C., Cervantes, B. & Dueber, J. E. A Highly Characterized Yeast Toolkit for Modular, Multipart Assembly. *ACS Synth. Biol.* **4**, 975–986 (2015).
25. Kelly, J. R. *et al.* Measuring the activity of BioBrick promoters using an in vivo reference standard. *J. Biol. Eng.* **3**, 4 (2009).